IEEE Access
Multidisciplinary ⋮ Rapid Review ⋮ Open Access Journal

Received 15 January 2024, accepted 17 February 2024, date of publication 22 February 2024, date of current version 1 March 2024.

Digital Object Identifier 10.1109/ACCESS.2024.3368872

RESEARCH ARTICLE

Multiple Channel LoRa-to-LEO Scheduling for Direct-to-Satellite IoT

FELIPE AUGUSTO TONDO[1], MOHAMMAD AFHAMISIS[2,3], (Member, IEEE), SAMUEL MONTEJO-SÁNCHEZ[4], (Senior Member, IEEE), ONEL LUIS ALCARAZ LÓPEZ[5], (Member, IEEE), MARIA RITA PALATTELLA[2], (Member, IEEE), AND RICHARD DEMO SOUZA[1], (Senior Member, IEEE)

[1]Department of Electrical and Electronics Engineering, Federal University of Santa Catarina, Florianópolis, Santa Catarina 88040-900, Brazil
[2]Luxembourg Institute of Science and Technology, 4362 Esch-sur-Alzette, Luxembourg
[3]Faculty of Science, Technology and Medicine, University of Luxembourg, 4365 Esch-sur-Alzette, Luxembourg
[4]Instituto Universitario de Investigación y Desarrollo Tecnológico, Universidad Tecnológica Metropolitana, Santiago 8940577, Chile
[5]Centre for Wireless Communications, University of Oulu, 90570 Oulu, Finland

Corresponding author: Felipe Augusto Tondo (felipe.tondo@posgrad.ufsc.br)

This work was supported in part by Coordenação de Aperfeiçoamento de Pessoal de Nível Superior (CAPES), Conselho Nacional de Desenvolvimento Científico e Tecnológico (CNPq), Brazil, under Grant 402378/2021-0, Grant 305021/2021-4, and Grant 40130/2022-0; in part by RNP/MCTIC 6G Mobile Communications Systems under Grant 01245.010604/2020-14; in part by Chile by Agencia Nacional de Investigación y Desarrollo (ANID) Fondo Nacional de Desarrollo Científico y Tecnológico (FONDECYT) Regular No. 1241977; in part by the Finland by the Academy of Finland (6G Flagship Program) under Grant 346208; in part by the Finnish Foundation for Technology Promotion; and in part by Luxembourg by the LORSAT Project through the National Research Fund Luxembourg (FNR) under Grant CORE/C19/IS/13705191.

ABSTRACT The exponential growth of Internet of Things (IoT) applications led to the deployment of IoT devices in remote areas beyond the reach of terrestrial networks, calling for satellite network solutions. Indeed, Low-Earth Orbit (LEO) satellites can provide global connectivity to direct-to-satellite (DtS)-IoT applications, with remarkable impact in several areas, as environmental monitoring, precision agriculture, and disaster prevention. One of the key challenges in DtS-IoT is supporting energy and spectral efficient multiple access, which has attracted a lot of attention recently. This work presents two novel multiple-access scheduling strategies for DtS-IoT networks, both inspired by the scheduling algorithm for LoRa to LEO satellites (SALSA). The latter prevents collisions by applying a first-come-first-served (FCFS) policy to allocate dedicated time slots according to the devices' rise times. However, the effectiveness of SALSA decreases in high-density scenarios, for which the visibility time of many devices is insufficient to successfully schedule their transmission. In the proposed scheduling methods, we take advantage of the availability of multiple frequency channels and the ability to change the transmission scheduling order of some devices within a visibility time window to improve uplink efficiency. The numerical results show that the average number of uplinks per lap and per visible device increases with the number of available channels, providing an improvement of almost 80% in terms of system uplink efficiency, and the proposed scheduling methods are more effective with smaller packet sizes. Additionally, we explore that the fusion of both scheduling strategies can further boost the system performance while guaranteeing an uplink efficiency greater than 50%, as elucidated across the implementation algorithms with four, six, and eight multiple channels.

INDEX TERMS Internet of Things (IoT), low-earth orbit (LEO) satellites, LoRa, medium access control, multiple channels.

I. INTRODUCTION

The future massive Machine Type Communication (MTC) solutions are expected to make our society more digital and interconnected [1]. The MTC market size is supposed

The associate editor coordinating the review of this manuscript and approving it for publication was Wei Feng.

to generate 12.6 trillion dollars by 2030, especially the numerous and novel Internet of Things (IoT) applications [2]. However, the realization of this anticipated flourishing market may be limited by challenges inherent to MTC. In this sense, future sixth-generation (6G) systems aim to overcome limitations of fifth-generation (5G) systems, such as device lifetime, implementation costs, communication reliability, and hardware complexity [3]. Nevertheless, such massive traffic volume in 6G could create other issues related to medium access, mobility management, traffic offloading, and interference in high-density areas [4]. Moreover, guaranteeing global connectivity for MTC applications requires non-terrestrial solutions [5], which are typically expensive.

The accessible costs for launching miniaturized Low-Earth Orbit (LEO) satellites have made Direct-to-Satellite (DtS)-IoT systems affordable and attractive. Low altitude ($\cong$ 160 $-$ 1000 km) satellites can guarantee low latency ($\cong$ 7 ms) and a convenient orbital period ($\sim$ 90 minutes) which favor the satellite revisit rate [6]. Sparse and dense constellations of near-Earth orbiting satellites can provide IoT connectivity on a global scale at a limited cost, covering large regions that remain unconnected [6], [7]. In short, DtS-IoT systems will be essential in various areas of development and sustainability, such as agriculture, meteorology, response to environmental disasters, and monitoring of flora and fauna [8], [9]. In addition, satellite-based IoT systems for remote monitoring can help avoid unnecessary expenses, for instance in public health, fisheries, tourism, and water management sectors [10].

Due to the numerous yet-to-discover applications towards 6G, non-terrestrial networks must be enhanced to provide, in addition to global connectivity, high quality of service (QoS) [11]. In this regard, medium access control (MAC) is a relevant research direction in DtS-IoT systems [12]. To improve the efficiency of non-terrestrial IoT networks, MAC protocols should consider the implementation complexity and the satellite trajectory. Among the topics related to MAC and orbital dynamics, the transmission scheduling of the devices should be highlighted, which is the topic addressed in this research work. In [13], the IoT devices transmit their data packets using LoRa technology [14] in allocated time slots to a gateway installed onboard the satellite. The transmission time slots are assigned to each IoT device using the scheduling algorithm for LoRa to LEO satellites (SALSA). When the first-come-first-serve (FCFS) policy is used in scenarios with a low density of ground nodes, the transmission of each device mostly coincides with the first instant in which the satellite is visible to that device.

However, following the FCFS policy, in a dense scenario, many devices may not be able to successfully transmit during the satellite visibility window due to excessive congestion. To address this drawback and inspired by [13], we present two novel low computational cost scheduling strategies for DtS-IoT networks. As a first novelty, we introduce the LoRa-to-LEO scheduling with permutation (L2L-P) of scheduled times. This strategy takes advantage of the ability to change the scheduling order of the IoT devices within the visibility time window and explore unused time by the previously proposed SALSA [13]. Furthermore, we present the LoRa-to-LEO with Alternating channels (L2L-A). A strategy that effortlessly re-distributes the order of IoT devices to optimize the efficient utilization of available channels. The numerical results show that combining both strategies in L2L-AP considerably improves the average number of uplinks, reaching nearly 95% of the system uplink efficiency when the IoT setup is over the area of France. This is a relevant improvement compared to the FCFS method, which achieves around 15% of the average uplinks per visible device in a dense scenario with 10^3 IoT devices.

Next, Section II discusses the related state-of-art literature and highlights the novelty of this work. Section III describes the system model, while Section IV formulates the proposed scheduling methods. Section V presents the simulation method and parameters, while Section VI discusses the simulation results. Finally, Section VII concludes the paper.

II. RELATED WORK

In recent years, great strides have been made in low-power wide area networks (LPWANs). The remarkable success of LoRa technology [14] redefined the concepts of long-range connectivity and low energy consumption, opening a new opportunity for IoT communication systems [13]. However, in particular cases, such as dense deployments or long transmission distances like in DtS-IoT scenarios, the LoRaWAN protocol [15] has some limitations [16]. This motivated a recently introduced variant in [17] that can improve throughput performance in very dense scenarios, but it is still not able to avoid collisions or operate with high energy efficiency.

A recent work [6] discusses some challenges in DtS-IoT related to the channel, the orbital dynamics, and the highly constrained IoT devices. The authors state that existing IoT MAC schemes need to be critically reviewed, especially those aiming to enable effective communication of thousands of devices with the gateway in a relatively short period. In large clusters, with many devices competing for data transmission opportunities during a satellite lap with an ALOHA-based protocol such as LoRaWAN, the probability of collision will be high, leading to problems in terms of scalability and energy efficiency [18]. Furthermore, with the advent of 5G communications and beyond, clustering algorithms aimed at reducing the complexity of resource allocation are appealing [19], particularly in dense DtS-IoT scenarios. A traffic allocation strategy for ALOHA networks was recently proposed in [20], which achieves non-zero throughput even in cases with very high traffic load but is very energy inefficient in this regime. In this sense, the authors [21] introduced LMAC, an efficient carrier-sense multiple access (CSMA) protocol designed for LoRa networks. This protocol aims to achieve a significant advancement in LoRa communications, promising a 2.2$\times$ improvement in performance and a substantial 2.4$\times$

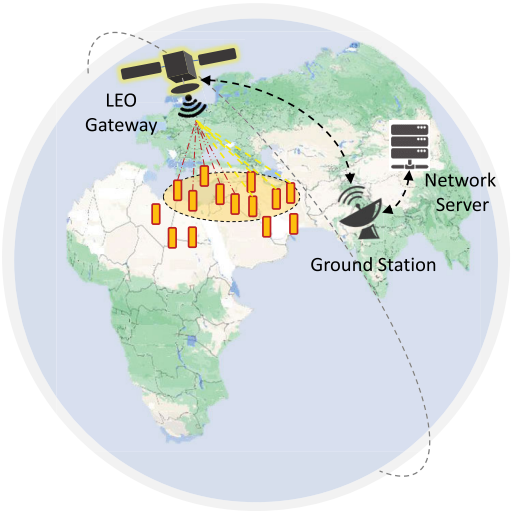

FIGURE 1. The DtS-IoT system, which comprises: a gateway in the LEO satellite, IoT devices spread over the target area, the network server, and the satellite ground station.

reduction in energy consumption compared to the ALOHA mechanism. Across three advancing versions of LMAC, this study attracts considerable interest in Direct-to-Satellite (DtS) scenarios, thanks to its implementation of channel load balancing based on the global locations of the IoT nodes and gateways.

In DtS-IoT, the choice of MAC protocol considerably affects the system performance in terms of throughput and energy efficiency [22]. Notice that the devices are spread over the footprint of the LEO satellite, with different visibility times, the MAC protocol can exploit this characteristic and optimize the uplink resources using appropriate device scheduling. Indeed, SALSA algorithm is based on the knowledge of the visibility times [13]. Specifically, time slots are assigned to each device based on those visibility times to avoid collisions and replication. Moreover, uplink policies and a mixed integer linear programming model to provide an upper bound in performance for scheduled LoRa-based DtS-IoT were proposed in [16]. In addition, the authors concluded that trajectory-based policies can duplicate the amount of served IoT nodes.

Departing from LoRa-based networks, a resource allocation scheme based on genetic algorithms for load balancing was provided in [23]. Therein, problems such as low efficiency in extremely non-uniform user distribution conditions and density variations were detected. In a similar line, but considering narrowband IoT, the authors in [24] proposed a scheduling pattern that maximizes a profit depending on data packet sizes, channel conditions, and satellite visibility time.

This paper considers the problem of scheduling the transmissions of IoT devices in a DtS-IoT system using LoRa technology. We adopt the same set-up of [13], but herein we include multiple frequency channels to simultaneously assume several transmissions corresponding to IoT nodes with similar visibility windows. In addition, we propose an efficient method to swap the time slots assigned to some devices based on their set times, thus creating new transmission opportunities for IoT devices that would not otherwise transmit. Furthermore, unlike the policies proposed in [16], our method generates a collision-free channel access strategy that can be implemented with low computational complexity, so it can even be run on-board the satellite if necessary. Finally, concerning [23], [24], our proposed approach is tailored for LoRa-based DtS-IoT networks, with low computational complexity and high effectiveness despite the dynamics of these scenarios.

Despite the acknowledged relevance of carrier sensing protocols like CSMA for LoRa technology [21], their current implementation is not entirely suitable for integration with DtS-IoT scenarios. Aspects such as the high probability of hidden nodes during satellite lap require further depth investigations [12], [26]. Ensuring comparative fairness between the proposed methods is quite a challenge, so this work does not focus on CSMA or even simple ALOHA policies. We specifically aim to improve the system uplink efficiency in the SALSA scenario.

III. SYSTEM MODEL

We consider an IoT network that operates within the coverage of an LEO satellite, where IoT devices are uniformly distributed in fixed locations within the target area and directly transmit data packets to the satellite in allocated time slots. We also assume that the devices utilize the LoRa communication technology [14]. Fig. 1 illustrates the scenario, with a cluster of IoT nodes on the ground communicating with a gateway on board the LEO satellite. The LEO satellite connects with a ground station that forwards the received packets to a network server (NS). Furthermore, the system dynamics are affected by orbit parameters, satellite footprint, and the target area, with each device having different visibility times during one satellite lap.

We denote the total number of satellite laps as M and the total number of IoT devices within the target area as N. Due to the system dynamics, each device appears and disappears from the satellite footprint at different times in each satellite lap. Such times are termed as rise-time $R_{m,n}$ and set-time $S_{m,n}$, for $m \in \{1, 2, \ldots, M\}$ and $n \in \{1, 2, \ldots, N\}$. Thus, each device n is visible for the satellite lap m during a time window defined by the interval $V_{m,n} = [R_{m,n}, S_{m,n}]$. Moreover, we assume that the IoT devices generate traffic with the same priority and always have information to transmit (full-buffer assumption), but can only transmit when they are within the satellite's footprint. The NS is responsible for scheduling collision-free uplink transmissions, at most one per device per lap, taking into account the visibility time of each IoT device. We assume a configuration for extended coverage with a spreading factor (SF) equal to 12 and 125 kHz bandwidth. Note that the required SF or bandwidth will depend on the orbit height and target area [27]. We consider the availability of multiple channels in our system model, which favors the

TABLE 1. LoRa airtime τ according to Spreading Factor SF = 12, Europe Region EU868, BW = 125 kHz.

Payload size (bytes)	$51-48$	$47-43$	$42-38$	$37-33$	$32-28$	$27-23$	$22-18$	$17-13$	$12-8$	$7-3$	$2-1$
τ (ms) [25]	2793.50	2629.60	2465.80	2302.00	2138.10	1974.30	1810.40	1646.60	1482.80	1318.90	1155.10

allocation of transmission resources in practical scenarios with numerous devices deployed in the target area. This approach is consistent with LoRa and allows more efficient utilization of visible time windows, which improves overall system performance. We denote as H the total number of available frequency channels.

The NS must consider the visibility times of each device and the time-on-air per packet (τ) to correctly schedule the uplinks. In Table 1, we list the value of τ for different payload sizes according to the regional parameters for Europe (EU868), based on [25]. Moreover, as in [13], we include two guard times $\delta = 10$ ms, before and after each transmission, to avoid collisions due to synchronization imperfections among devices and the satellite. Thus, the NS reserves the channel for each uplink transmission considering the total time, which comprises two guard times δ and the packet τ.

Following SALSA [13], the scheduled beginning time for the uplink of the n^{th} device in the m^{th} lap, denoted as $B_{m,n}$, is defined by the NS and depends on: *i*) the orbit dynamics; *ii*) the number of devices within the satellite footprint. A transmission from another device on the same channel is only scheduled after the end transmission time ($E_{m,n}$) of the device previously scheduled. In other words, a transmission window corresponding to the interval $T_{m,n} = \left[B_{m,n}, E_{m,n}\right]$ is allocated only for the n^{th} device during the m^{th} lap.

IV. THE PROPOSED SCHEDULING METHODS

Next, we describe the proposed scheduling approaches for DtS-IoT. The methods are based on the SALSA-FCFS policy [13], which works in a first-come-first-serve fashion. In SALSA-FCFS, the first device to appear in the satellite footprint is the first to transmit, and so on (*i.e.*, the scheduling queue is based on the respective rise-times). Initially, as in [13], let us consider the availability of a single-frequency channel. The operation of SALSA-FCFS is illustrated next.

Example 1: Let us assume $N = 4$ devices want to transmit payloads of 51 bytes (the maximum with SF12). Their rise-times $R_{m,n}$ and set-times $S_{m,n}$ are illustrated in Fig. 2a. Following the SALSA-FCFS policy, the scheduled transmissions are represented by boxes whose boundaries correspond to the beginning-times $B_{m,n}$ and end-times $E_{m,n}$ for each allocated device uplink. Moreover, the guard times are highlighted in blue. Note that the 4^{th} device is denied transmission as its remaining visibility time after the transmission of the three devices that came first (these are the ones that entered the satellite footprint first and have the lowest rise times) is not sufficient to accommodate the total time for that payload size.

Note that assigning uplinks based solely on rise times does not guarantee to scheduling as many transmissions as possible, due to the differences in the duration of the visibility window of the devices given their locations and the satellite footprint. On the other hand, scheduling uplink transmissions by the longest set time of each device, or first-leave-first-serve (FLFS) allocation, would be unfair and inefficient because it would not take advantage of the timely arrival of many IoT devices. Next, we introduce a strategy that seeks to create additional transmit opportunities after the application of the FCFS policy.

A. PERMUTATION OF SCHEDULED TIMES: L2L-P

In SALSA-FCFS, a device with a short visibility time may have very few opportunities to transmit unless it is one of the first to appear in the footprint. The situation gets worse with the network density, as many devices may have intersecting visibility times. Add to that the fact that the duration of the visibility times may be considerably different among devices. To deal with these problems, we consider the permutation of the scheduled times from the initial SALSA-FCFS scheduling [13], looking for the reallocations that allow scheduling uplinks discarded by the FCFS policy.

Algorithm 1 describes in detail the implementation of the proposed LoRa-to-LEO with Permutation of scheduled times (L2L-P) approach in the m^{th} lap. Algorithm inputs include the rise and set times based on the relative locations of the devices concerning the satellite orbit, as well as transmission beginning and end times scheduled by the SALSA-FCFS schedule. We define $\mathbb{V}_m = \{V_{m,1}, \cdots, V_{m,N}\}$ as the set whose elements are the visibility time intervals of each device in that lap. The algorithm checks which devices are allocated a transmit window considering the SALSA-FCFS policy, and constructs the set $\mathbb{T}_m = \{T_{m,1}, \cdots, T_{m,N}\}$ containing the intervals corresponding to the allocated time windows for each device. At this point, we can determine the time intervals (if any) not allocated to any device, which are listed in the free time set $\mathbb{F}_m$. Furthermore, the users are separated into two sets: $\mathbb{J}_m$, containing the joined or scheduled devices, and $\mathbb{D}_m$, with the discarded or unscheduled devices in that lap.

Considering the devices $n \in \mathbb{J}_m$, the L2L-P algorithm calculates $\Omega = \max S_{m,n} - \max E_{m,n}$, *i.e.*, it determines the amount of time Ω not used by FCFS after the transmission of the last scheduled uplink ($\max E_{m,n}$) and that is visible by at least one device ($\max S_{m,n}$). Note that at most $p = \lfloor \frac{\Omega}{2\delta+\tau} \rfloor$ devices from $\mathbb{J}_m$ could be reallocated to this unused time, opening transmit opportunities for devices within $\mathbb{D}_m$. Next, if $p \geq 1$, the devices in $\mathbb{J}_m$ with $S_{m,n} > \max E_{m,n}$ are included in set $\mathbb{P}_m$ and they are ordered in decreasing $S_{m,n}$. The first device in $\mathbb{P}_m$ is reallocated to the end of the visibility window

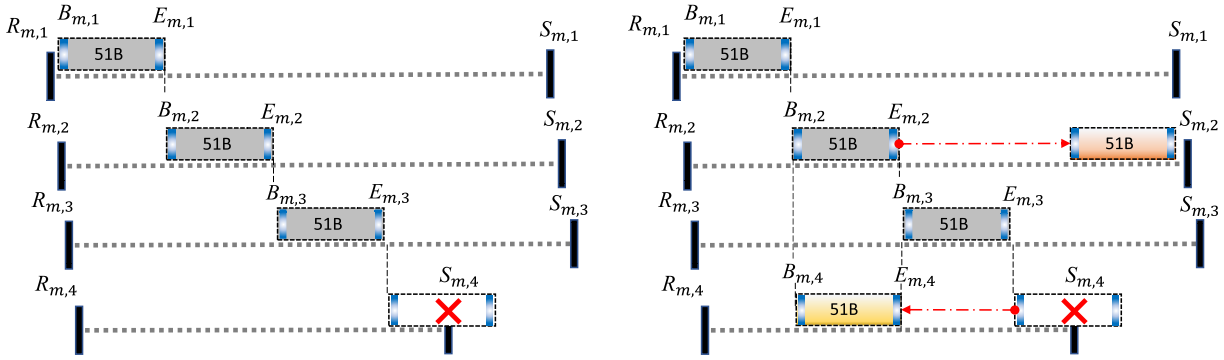

FIGURE 2. Uplink schedules in the m^{th} lap, including rise-time $R_{m,n}$, set-time $S_{m,n}$, beginning-time $B_{m,n}$, end-time $E_{m,n}$, and guard times (in blue). (a) SALSA-FCFS, where the 4$^{\text{th}}$ device could not be scheduled (left). (b) L2L-P, where the uplink of the 2$^{\text{nd}}$ device is rescheduled so that the 4$^{\text{th}}$ device can transmit (right).

so that its new $E'_{m,n}$ becomes $S_{m,n}$. The previously allocated time interval for this device moves from $\mathbb{T}_m$ to $\mathbb{F}_m$. Next, p is decremented, and if it is still larger or equal to 1, the algorithm checks if the next device in $\mathbb{P}_m$ can be reallocated, so that its set time is as close as possible to the beginning transmission time of the previously reallocated device, and so on.

Next, for each device in $\mathbb{D}_m$, the algorithm checks if its visibility time interval $V_{m,n}$ has an intersection greater than or equal to $(2\delta + \tau)$ with any element in $\mathbb{F}_m$. If so, the transmission of that n^{th} IoT device is scheduled within the idle interval found in the most efficient way (*i.e.*, by matching $B_{m,n}$ with the left edge of the free time interval or $E_{m,n}$ with the right edge of the free time interval). Then, the scheduled transmission $T_{m,n}$ is removed from $\mathbb{F}_m$ and is included in $\mathbb{T}_m$. At the end of this procedure, up to p IoT devices from $\mathbb{D}_m$ may be moved to $\mathbb{J}_m$, increasing the uplink efficiency.

Example 2: Consider the case discussed in Example 1 and Fig. 2a, where the 4th IoT device was not scheduled. However, if we move the 2nd IoT device's uplink to the idle time interval after the 3rd device's uplink, then the 4th device's uplink can be scheduled at the time interval that was previously reserved for the 2nd device. Thanks to this rescheduling, the uplinks of the four devices can be scheduled, as illustrated in Fig. 2b.

Example 3: As an additional illustration of the L2L-P operation, Fig. 3 shows the visibility time windows $V_{m,n}$ for 250 devices under the coverage of a satellite. First, the SALSA-FCFS allocation was applied, resulting in the sequential schedule illustrated with different marker colors in Fig. 3. Note that the uplinks are ordered by rise times, while several IoT devices (whose visibility windows were represented by red dots) are not initially scheduled due to their set times. However, after running the L2L-P algorithm, some of the allocated devices have their transmit times shifted to the end of the overall visibility window (the new uplinks of these devices are marked in green in Fig. 3, making room for other devices that could not transmit before (these uplinks are identified with big red dots in Fig. 3). Thus, the uplink efficiency can be improved concerning the FCFS strategy.

Algorithm 1 L2L-P

Input: $R_{m,n}$, $S_{m,n}$, $B_{m,n}$, $E_{m,n}$, τ, δ, m;
Construct: $\mathbb{V}_m$, $\mathbb{T}_m$, $\mathbb{F}_m$, $\mathbb{J}_m$, $\mathbb{D}_m$;
Initialize: $i = 1$, $B'_m = \emptyset$;
Calculate: $\Omega = \max S_{m,n} - \max E_{m,n}$, $p = \lfloor \frac{\Omega}{2\delta+\tau} \rfloor$;
if $p \geq 1$ **then**
  Construct $\mathbb{P}_m$ and order devices in decreasing $S_{m,n}$;
  while $p \geq 1$ **do**
    Find: $n \in \mathbb{P}_m(i)$;
    $E'_{m,n} = \min(B'_m, S_{m,n})$;
    $B'_{m,n} = E'_{m,n} - (2\delta + \tau)$;
    Include $T_{m,n}$ in $\mathbb{F}_m$ and remove it from $\mathbb{T}_m$;
    $T_{m,n} = [B'_{m,n}, E'_{m,n}]$;
    Include $B'_{m,n}$ in B'_m;
    Include $T_{m,n}$ in $\mathbb{T}_m$;
    $i = i + 1$;
    $p = p - 1$;
  end while
  for each $n \in \mathbb{D}_m$ **do**
    $I_{m,n} = V_{m,n} \cap \mathbb{F}_m$
    if $I_{m,n} \geq 2\delta + \tau$ **then**
      $T_{m,n} = I_{m,n}$ (left aligned);
      Include $T_{m,n}$ in $\mathbb{T}_m$;
    end if
  end for
end if
Output: Allocated time windows $\mathbb{T}_m$.

The above discussion and examples consider a single channel. Next, we present a strategy that can efficiently allocate the devices when multiple channels are available, which further leverages the potential of the L2L-P algorithm.

B. EXPLOITING MULTIPLE CHANNELS: L2L-A AND L2L-AP

We design a scheduling strategy that considers the availability of H orthogonal frequency channels. First, the visible devices in the m^{th} lap are divided into H uplink groups. For that sake,

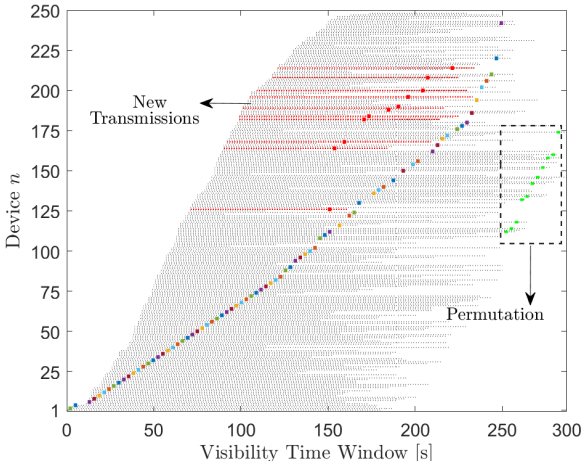

FIGURE 3. Visibility time window and scheduling for 250 devices using the L2L-P algorithm in a single channel scenario.

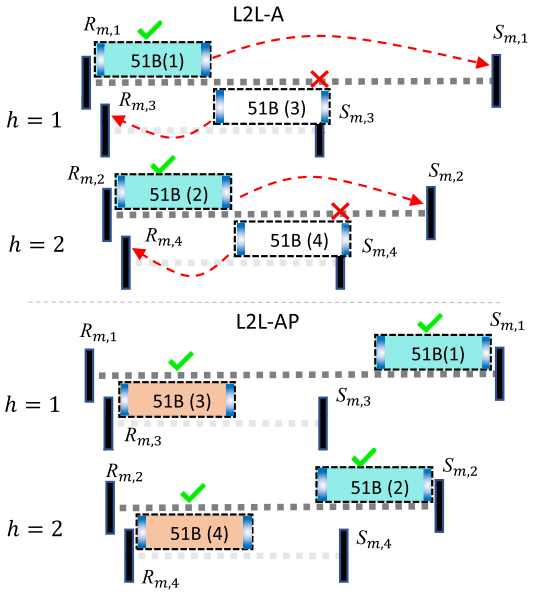

FIGURE 4. Uplink schedules in the m^{th} lap, including rise-time $R_{m,n}$, set-time $S_{m,n}$, beginning time $B_{m,n}$, end time $E_{m,n}$, and guard times (in blue). Devices 1 and 3 transmit in channel $h = 1$, while devices 2 and 4 transmit in channel $h = 2$. The red arrows indicate the permutation operation.

we first order the devices according to their rise times $R_{m,n}$. We then assign the devices to the groups alternately, such that the device with the first (second) rise time is assigned to the first (second) group, and so on. This first group will include all those devices located in positions multiple of H plus 1 (which will be serviced from the first channel). Devices in positions that are multiple of H plus h will belong to the h^{th} group and will be served from the h^{th} channel. After the devices are separated into the H groups, the FCFS policy is applied in each group, yielding the transmitting time slots allocated for each group. The above strategy is the LoRa-to-LEO with Alternating channels (L2L-A) algorithm, which guarantees an efficient distribution of all IoT devices according to their respective rise times.

The permutation strategy described in the previous section can be applied to each group, thus increasing the number of scheduled uplinks on each channel. We refer to the application of the L2L-A method followed by the L2L-P strategy in each channel as the novel scheduling policy named L2L-AP, which is illustrated next.

Example 4: Consider the case illustrated in Fig. 4, with $N = 4$ devices. If the devices were to be allocated in a single channel, using either SALSA-FCFS or L2L-P, it would not be possible for all to transmit in the same satellite lap. However, assuming there are two available channels, a more favorable allocation can be defined. Following the L2L-A logic, since there are $H = 2$ channels, devices 1 and 3 would be in the first group (they transmit in the first channel) and devices 2 and 4 would be in the second group (they transmit in the second channel). But even with channel allocation devices 3 and 4 would not be able to transmit. However, if after L2L-A we apply the L2L-P approach in each of the two channels, which leads to the L2L-AP algorithm, then the final allocation is as illustrated in Fig. 4, in which device 3 is the first one to transmit in channel 1, followed by device 1. In channel 2, device 4 is the first to transmit, followed by device 2.

Algorithm 2 summarize the steps of the L2L-A and L2L-AP strategies, respectively. The multi-channel approaches not only increase the number of uplink transmissions by exploiting the multiple available channels, but also increases the benefits associated with permutation since ordered and unsaturated use of each channel is more efficient. This makes the L2L-AP approach very efficient in terms of uplink resources.

Remark 1: Note that the input of L2L-AP is the output of L2L-A. Then, L2L-AP looks for potential uplink permutations to open up opportunities for unscheduled devices. Therefore, L2L-AP never performs worse than L2L-A.

Remark 2: Given the orbit dynamics and the position of the devices, it may happen that the visibility times set $\mathbb{V}_m$ can be decomposed into two or more disjoint subsets. In such cases, the algorithms proposed in this section must be executed on each of these subsets separately.

Remark 3: Note that the allocation of time slots could be carried out using an optimization problem similar to that in [16]. However, such a solution is not scalable as it becomes prohibitive given the increase in its complexity with the increase in the number of IoT devices. In this work, we focus on low-complexity and highly efficient scheduling methods, which could be even executed on-board the LEO satellite if necessary and if the network server is also implemented onboard.

C. PRACTICAL CONSIDERATIONS

For a practical implementation of the proposed method, the network server or system coordinator must know the trajectory of the LEO satellite and the location of the IoT devices. First, we note that satellite visibility can be predicted with great accuracy using techniques from the perspective

Algorithm 2 Multi-Channel LoRa-to-LEO Scheduling

Input: $R_{m,n}$, $S_{m,n}$, τ, δ, H;
Split the visible devices into H sub-groups;
Choose: L2L-A (a) or L2L-AP (b);
for each $h \in H$ **do**
  if (a) **then**
    Allocate time windows $T_{m,n}$ using SALSA-FCFS;
  else if (b) **then**
    Allocate time windows $T_{m,n}$ using SALSA-FCFS;
    Apply the L2L-P algorithm;
  end if
end for
Output: Allocated time windows $\mathbb{T}_m$ per channel.

of either the LEO satellite [28], [29], [30] or the ground nodes [31], [32], [33]. Furthermore, the location of the devices can be informed to the network server during the installation and registration of each IoT device. For example, the latitude and longitude information is an input of the popular The Things Network server [34]. Therefore, the assumption of known ground devices' location and satellite trajectory on the network server is reasonable for scenarios with static IoT devices, thus constituting a constraint in the proposed system model. Moreover, the computation of the scheduling times can be executed at the Earth station and transmitted to the satellite, which then could inform the devices in the downlink phase, using acknowledgment messages for class A or a synchronization beacon for class B devices. Directly related to the above considerations, it is relevant to mention that a hybrid emulation-based testbed with real LoRa devices using the baseline FCFS SALSA strategy has been successfully tested [35], confirming its practical feasibility.

The network performance in DtS-IoT is vulnerable to potential wireless interference, including mutual interference between users [16], [36]. Additionally, uplink transmission may be impacted by other sources. However, Semtech studies [37] have announced the feasibility of LPWANs co-existing harmoniously with other high-power systems that generate frequency-selective interference. In our focus, the efforts are directed toward enhancing uplink efficiency. Finally, another potential issue of concern for practical deployments is that DtS-IoT communications are susceptible to the Doppler effect [24] due to satellite movement. However, recent experiments based on LoRa technology revealed a minimum performance impact from the Doppler effect considering LEO satellites [38], [39]. Therefore, in line with the related literature [13], [16], [18], we do not consider this effect in this work as its practical implication should be minimal.

V. SIMULATION METHOD AND PARAMETERS

A computer simulation is deployed to evaluate the proposed scheduling methods in a realistic DtS-IoT scenario, following

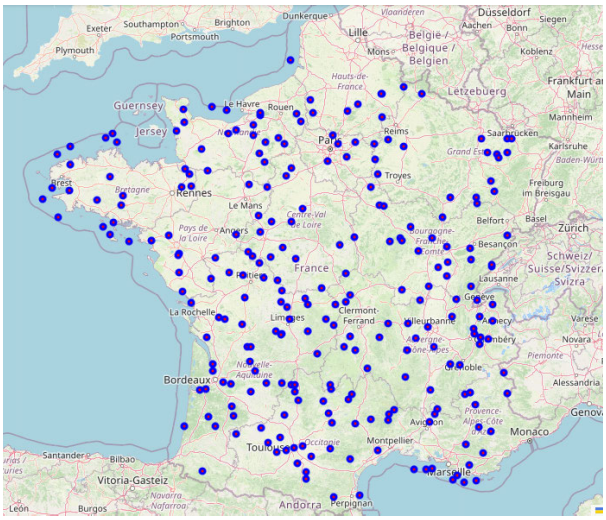

FIGURE 5. Deployment of 250 IoT devices (blue circles) in France, covered by LacunaSat-3.

the approach in SALSA [40], where the location of the N devices is randomly generated within a region. Then, we extract the location of each device on the ground, in terms of latitude and longitude, using geocoders from the Python GeoPy library [41]. Satellite visibility times of IoT devices are estimated using the Python Skyfield astronomy library [42]. This library uses public data information in the two-line element (TLE) set format, available from the CelesTrack platform [43], for determining the locations of the satellite according to the orbit and pointing time. Thus, the IoT devices are deployed in the target area, their visibility times are determined in each satellite lap, and the different scheduling strategies are evaluated. Such evaluation, analysis, and visualization of the results are carried out in MatLab®.

In this work, we consider the region delimited by the borders of France for deploying the devices. France is well distributed in all directions, ranging around 1000 km north to south and east to west, so the visibility times of the IoT devices may be considerably different depending on the orbit dynamics. We consider different numbers of devices spread over the target area, from $N = 100$ to $N = 1000$. Using the OpenStreetMap library, Fig. 5 illustrates one deployment of 250 devices in France. Moreover, we consider the real orbit of the LacunaSat-3 LEO satellite, with a height of 500 km to 600 km from the Earth and a minimum elevation angle of 30°, as in [7] and [13], to determine the satellite footprint. In addition, we assume different numbers of channels, $H \in \{1, 2, 4, 6, 8\}$. Finally, the results consider a period of 31 days in March 2023.

VI. NUMERICAL RESULTS

In this section, we evaluate the performance of the proposed scheduling methods. Fig. 6 shows the number of uplinks per lap for $N = 1000$ devices in the target area. The red line indicates the number of visible devices per lap, which is also the upper bound of the number of uplinks per lap.

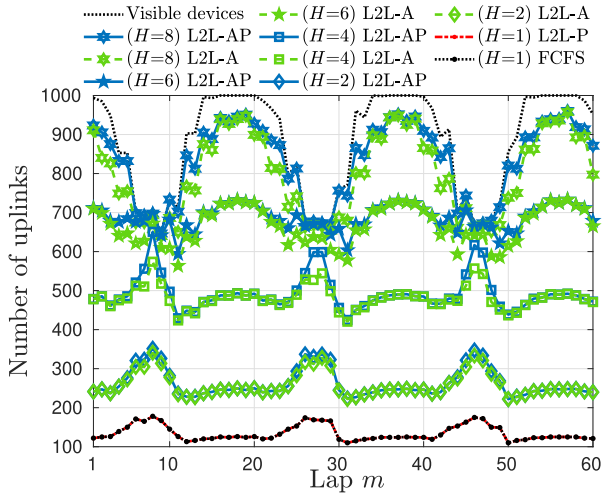

FIGURE 6. Number of uplinks per lap for $N = 1000$ devices and $H \in \{1, 2, 4, 6, 8\}$ channels.

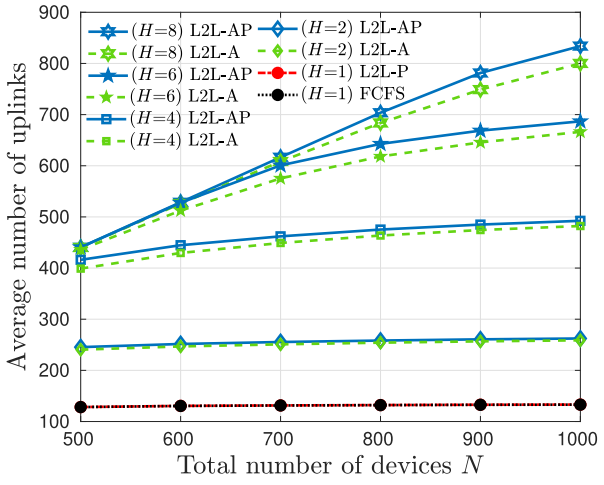

FIGURE 7. The average number of uplinks per lap as a function of the total number of IoT devices.

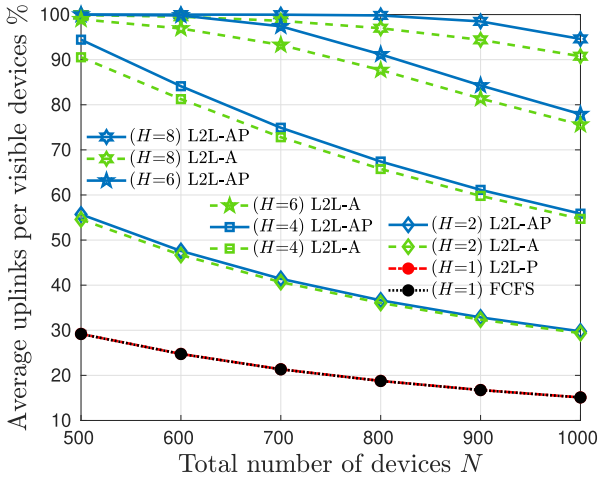

FIGURE 8. The average number of uplinks per visible device as a function of the total number of IoT devices.

As expected, increasing the number of channels allows more devices to transmit, while the margin by which L2L-AP outperforms L2L-A increases with H too. Moreover, in laps with few visible devices but sufficient visibility time, L2L-AP with $H = 4$ achieves almost the same performance as L2L-A with $H = 6$ channels. To understand this phenomenon, let us focus on lap $m = 8$. Although not shown here, in this lap the set of visible IoT devices can be divided into two subsets of disjoint visibility windows (see Remark 2), with similar numbers of devices per subset. Moreover, the sum of the visibility times of both subsets in lap $m = 8$ (505 seconds) is greater than the overall visibility time window of lap $m = 1$ (344 seconds), while the individual visibility windows of the devices in lap $m = 1$ have a very large intersection. Such scenarios with a large number of visible devices but somewhat limited visibility time for their allocation, as in lap $m = 1$, can only be efficiently served when many channels are available. That is why L2L-AP with $H = 8$ channels is very efficient, allowing almost all visible devices to transmit in any lap. Additionally, the performances of the L2L-P and FCFS scheduling strategies are illustrated in the red and black lines.

Fig. 7 shows the average number of uplinks per lap, considering 10 different deployments in the target area and $N \in \{500, 600, 700, 800, 900, 1000\}$ devices. Note that for $N = 500$, both L2L-A and L2L-AP have similar performance, between 300 and 400 uplinks. However, as the number of devices increases, the relative difference between the strategies and the number of channels becomes more visible. In particular, with $N = 1000$ devices and $H = 8$ channels, L2L-AP shows the best performance. Also note that the number of uplinks does not match the total number of devices, because the number of visible devices per lap is often less than the total number of devices in the target area.

Note that FCFS in Fig. 7 almost does not change its performance since for this particular payload size, guard times, orbit parameters, and target region, the maximum number of uplinks that SALSA-FCFS can schedule is less than 150. Considering only one channel, although the L2L-P method outperforms SALSA-FCFS in each lap, the average number of uplinks does not modify significantly. Long transmission queues are generated in single-channel systems when multiple IoT devices enter the satellite footprint simultaneously, which causes the maximum uplink capacity to be reached quickly. Note that the upper bound of the number of uplinks of a channel in the m^{th} lap can be estimated by considering the minimum rise time and the maximum set time of all the IoT devices, as well as the payload size and guard times, according to $\left(\max_n \left(S_{m,n}\right) - \min_n \left(R_{m,n}\right)\right)/(2\delta + \tau)$. Therefore, increasing the number of IoT devices will not lead to more transmission opportunities if the maximum capacity has already been reached for the lap in question. In addition, we also analyzed the performance of the proposed methods in terms of the system uplink efficiency, defined as the average number of uplinks per visible device, as illustrated in Fig. 8.

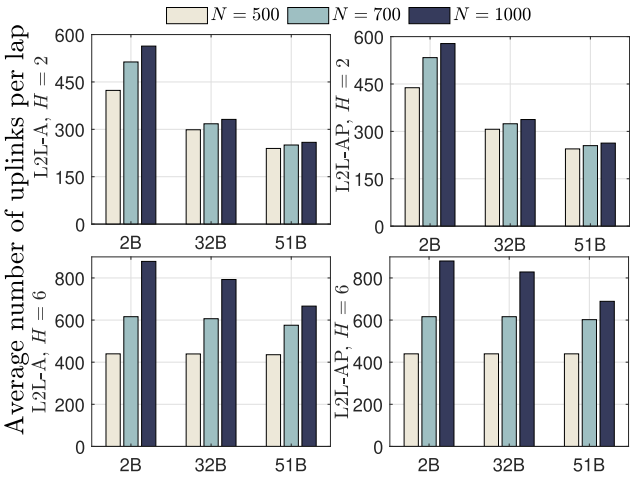

FIGURE 9. The average number of uplinks per lap for L2L-A (left) and L2L-AP (right) with two (top) and four (bottom) channels, considering different payload sizes (2B, 32B, and 51B) and $N \in \{500, 700, 1000\}$ IoT devices.

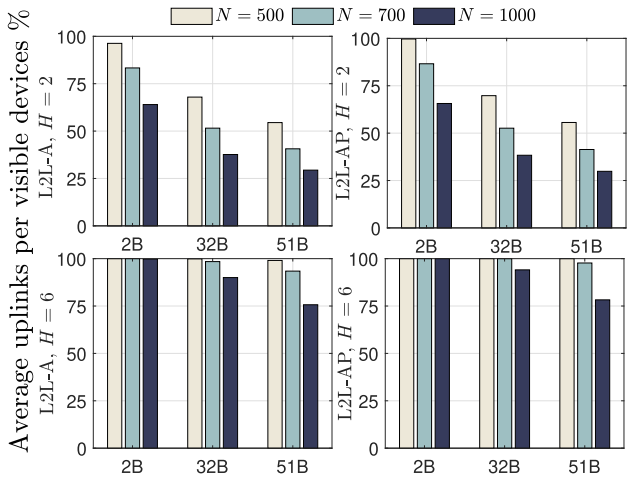

FIGURE 10. The average number of uplinks per visible device for L2L-A (left) and L2L-AP (right) with two (top) and four (bottom) channels, considering different payload sizes (2B, 32B, and 51B) and $N \in \{500, 700, 1000\}$ IoT devices.

The results complement those in Fig. 7, confirming that the proposed approaches exploiting multiple channels can considerably increase the uplink efficiency by approximately five times, representing an improvement of about 80% in a dense scenario with 10^3 IoT devices. Furthermore, Fig. 8 also guarantees an uplink efficiency greater than 50%, applying the scheduling algorithms with four, six, and eight multiple channels.

Finally, we investigate the impact of the payload size on the performance of the proposed methods. In Fig. 9, we show the average number of uplinks per lap for different numbers of channels, devices, and payload sizes. As expected, a smaller payload size leads to a lower τ, so more uplinks can be scheduled within the visibility time window. This effect is best appreciated in the case of $H = 2$ channels. We can see that the advantage of the L2L-AP over L2L-A increases with the number of available channels H, especially for larger payload sizes. Note that the average number of uplinks per lap does not match the number of devices because not all devices are visible at all laps due to the orbit dynamics and the position of the devices. In Fig. 10, we show the average number of uplinks per visible device that are scheduled when running L2L-A and L2L-AP with two or six channels for different numbers of devices and payload sizes. We can see that the proposed methods can achieve maximum efficiency in several setups. The highest uplink efficiencies are achieved with small payload sizes and the largest number of channels available. Finally, L2L-AP outperforms L2L-A in all configurations.

VII. CONCLUSION

We presented two novel scheduling approaches to be used in a DtS-IoT network. The L2L-A algorithm is particularly tailored to exploit multiple frequency channels efficiently. Meanwhile, the L2L-AP algorithm incorporates the possibility of swapping the time slots of already allocated devices, making room for new transmission opportunities. The numerical results demonstrate that the proposed methods can considerably improve the uplink efficiency of DtS-IoT networks, even in dense scenarios. In future work, we intend to consider segmentation of the payload to take advantage of short unused times within a lap and the parallel transmission of a message. In addition, we aspire to explore the pros and cons of the proposed methods using SALSA versus multi-channel LoRa-to-LEO scheduling for a real testbed.

REFERENCES

[1] N. H. Mahmood. (2020). *White Paper on Critical and Massive Machine Type Communication Towards 6G*. 6G Research Visions. Univ. Oulu. [Online]. Available: http://urn.fi/urn

[2] Axios Future. (2030). *Internet of Things Projected to Generate Up to 12.6 Trillion by 2030*. Accessed: Jul. 26, 2023. [Online]. Available: https://www.axios.com

[3] M. R. Mahmood, M. A. Matin, P. Sarigiannidis, and S. K. Goudos, "A comprehensive review on artificial intelligence/machine learning algorithms for empowering the future IoT toward 6G era," *IEEE Access*, vol. 10, pp. 87535–87562, 2022.

[4] V. D. P. Souto, P. S. Dester, M. S. P. Facina, D. G. Silva, F. A. P. de Figueiredo, G. R. de Lima Tejerina, J. C. S. S. Filho, J. S. Ferreira, L. L. Mendes, R. D. Souza, and P. Cardieri, "Emerging MIMO technologies for 6G networks," *Sensors*, vol. 23, no. 4, p. 1921, Feb. 2023, doi: 10.3390/s23041921.

[5] J. Kua, S. W. Loke, C. Arora, N. Fernando, and C. Ranaweera, "Internet of Things in space: A review of opportunities and challenges from satellite-aided computing to digitally-enhanced space living," *Sensors*, vol. 21, no. 23, p. 8117, Dec. 2021.

[6] J. A. Fraire, O. Iova, and F. Valois, "Space-terrestrial integrated Internet of Things: Challenges and opportunities," *IEEE Commun. Mag.*, vol. 60, no. 12, pp. 64–70, Dec. 2022.

[7] I. Leyva-Mayorga, B. Soret, M. Röper, D. Wübben, B. Matthiesen, A. Dekorsy, and P. Popovski, "LEO small-satellite constellations for 5G and beyond-5G communications," *IEEE Access*, vol. 8, pp. 184955–184964, 2020.

[8] J. A. Fraire, S. Henn, F. Dovis, R. Garello, and G. Taricco, "Sparse satellite constellation design for LoRa-based direct-to-satellite Internet of Things," in *Proc. IEEE Global Commun. Conf. (GLOBECOM)*, Dec. 2020, pp. 1–6.

[9] N. Saeed, A. Elzanaty, H. Almorad, H. Dahrouj, T. Y. Al-Naffouri, and M.-S. Alouini, "CubeSat communications: Recent advances and future challenges," *IEEE Commun. Surveys Tuts.*, vol. 22, no. 3, pp. 1839–1862, 3rd Quart., 2020.

[10] J. Morón-López, M. C. Rodríguez-Sánchez, F. Carreño, J. Vaquero, Á. G. Pompa-Pernía, M. Mateos-Fernández, and J. A. P. Aguilar, "Implementation of smart buoys and satellite-based systems for the remote monitoring of harmful algae Bloom in inland waters," *IEEE Sensors J.*, vol. 21, no. 5, pp. 6990–6997, Mar. 2021.

[11] M. M. Azari, S. Solanki, S. Chatzinotas, O. Kodheli, H. Sallouha, A. Colpaert, J. F. M. Montoya, S. Pollin, A. Haqiqatnejad, A. Mostaani, E. Lagunas, and B. Ottersten, "Evolution of non-terrestrial networks from 5G to 6G: A survey," *IEEE Commun. Surveys Tuts.*, vol. 24, no. 4, pp. 2633–2672, 4th Quart., 2022.

[12] T. Ferrer, S. Céspedes, and A. Becerra, "Review and evaluation of MAC protocols for satellite IoT systems using nanosatellites," *Sensors*, vol. 19, no. 8, p. 1947, Apr. 2019.

[13] M. Afhamisis and M. R. Palattella, "SALSA: A scheduling algorithm for LoRa to LEO satellites," *IEEE Access*, vol. 10, pp. 11608–11615, 2022.

[14] Semtech. (2023). *LoRa and LoRaWAN: A Technical Overview*. Accessed: Jul. 26, 2023. [Online]. Available: https://www.semtech.com/lora

[15] *LoRaWAN 1.1 Specification*, LoRa Alliance, San Ramon, CA, USA, Oct. 2017.

[16] G. Álvarez, J. A. Fraire, K. A. Hassan, S. Céspedes, and D. Pesch, "Uplink transmission policies for LoRa-based direct-to-satellite IoT," *IEEE Access*, vol. 10, pp. 72687–72701, 2022.

[17] LoRa Alliance. (2020). *RP2-1.0.2 LoRaWAN Regional Parameters*. Accessed: Jul. 26, 2023. [Online]. Available: https://lora-alliance.org/resourcehub/rp2-102-lorawan-regional-parameters/

[18] R. Ortigueira, J. A. Fraire, A. Becerra, T. Ferrer, and S. Céspedes, "RESS-IoT: A scalable energy-efficient MAC protocol for direct-to-satellite IoT," *IEEE Access*, vol. 9, pp. 164440–164453, 2021.

[19] A. Mukherjee, D. K. Jain, and L. Yang, "On-demand efficient clustering for next generation IoT applications: A hybrid NN approach," *IEEE Sensors J.*, vol. 21, no. 22, pp. 25457–25464, Nov. 2021.

[20] F. A. Tondo, V. D. P. Souto, O. L. Alcaraz López, S. Montejo-Sánchez, S. Céspedes, and R. D. Souza, "Optimal traffic load allocation for aloha-based IoT LEO constellations," *IEEE Sensors J.*, vol. 23, no. 3, pp. 3270–3282, Feb. 2023.

[21] A. Gamage, J. Liando, C. Gu, R. Tan, M. Li, and O. Seller, "LMAC: Efficient carrier-sense multiple access for LoRa," *ACM Trans. Sensor Netw.*, vol. 19, no. 2, pp. 1–27, May 2023.

[22] P. I. Parra, S. Montejo-Sánchez, J. A. Fraire, R. D. Souza, and S. Céspedes, "Network size estimation for direct-to-satellite IoT," *IEEE Internet Things J.*, vol. 10, no. 7, pp. 6111–6125, Apr. 2023.

[23] W. Lin, Z. Dong, K. Wang, D. Wang, Y. Deng, Y. Liao, Y. Liu, D. Wan, B. Xu, and G. Wu, "A novel load balancing scheme for satellite IoT networks based on spatial–temporal distribution of users and advanced genetic algorithms," *Sensors*, vol. 22, no. 20, p. 7930, Oct. 2022.

[24] O. Kodheli, N. Maturo, S. Chatzinotas, S. Andrenacci, and F. Zimmer, "NB-IoT via LEO satellites: An efficient resource allocation strategy for uplink data transmission," *IEEE Internet Things J.*, vol. 9, no. 7, pp. 5094–5107, Apr. 2022.

[25] The Things Network. (2023). *LoRaWAN Airtime Calculator*. Accessed: Jul. 26, 2023. [Online]. Available: https://www.thethingsnetwork.org/airtime-calculator

[26] S. Herrería-Alonso, M. Rodríguez-Pérez, R. F. Rodríguez-Rubio, and F. Pérez-Fontán, "Improving uplink scalability of LoRa-based direct-to-satellite IoT networks," *IEEE Internet Things J.*, vol. 10, no, 20, p. C4, Oct. 2023, doi: 10.1109/JIOT.2023.3333934.

[27] The Things Network. *Modulation & Data Rate*. Accessed: Jul. 26, 2023. [Online]. Available: https://www.thethingsnetwork.org/docs/lorawan/modulation-data-rate/

[28] H. Wang, C. Han, and X. Sun, "Analytical field-of-regard representation for rapid and accurate prediction of agile satellite imaging opportunities," *J. Astronomical Telescopes, Instrum., Syst.*, vol. 5, no. 3, Jun. 2019, Art. no. 037001.

[29] C. Han, Y. Zhang, S. Bai, X. Sun, and X. Wang, "Novel method to calculate satellite visibility for an arbitrary sensor field," *Aerosp. Sci. Technol.*, vol. 112, May 2021, Art. no. 106668.

[30] S. Bai, Y. Zhang, and Y. Jiang, "Minimum-observation method for rapid and accurate satellite coverage prediction," *GPS Solutions*, vol. 26, no. 4, p. 110, Oct. 2022.

[31] C. Han, X. Gao, and X. Sun, "Rapid satellite-to-site visibility determination based on self-adaptive interpolation technique," *Sci. China Technol. Sci.*, vol. 60, no. 2, pp. 264–270, Feb. 2017.

[32] C. Han, P. Yang, X. Wang, and S. Liu, "A fast computation method for the satellite-to-site visibility," in *Proc. IEEE Congr. Evol. Comput. (CEC)*, Jul. 2018, pp. 1–8.

[33] Y. Gu, C. Han, and X. Wang, "A Kriging based framework for rapid satellite-to-site visibility determination," in *Proc. IEEE 10th Int. Conf. Mech. Aerosp. Eng. (ICMAE)*, Jul. 2019, pp. 262–267.

[34] The Things Network. *The Things Network Console*. Accessed: Nov. 24, 2023. [Online]. Available: https://console.cloud.thethings.network/

[35] M. Afhamisis, S. Barillaro, and M. R. Palattella, "A testbed for LoRaWAN satellite backhaul: Design principles and validation," in *Proc. IEEE Int. Conf. Commun. Workshops (ICC Workshops)*, May 2022, pp. 1171–1176.

[36] F. A. Tondo, S. Montejo-Sánchez, M. E. Pellenz, S. Céspedes, and R. D. Souza, "Direct-to-satellite IoT slotted Aloha systems with multiple satellites and unequal erasure probabilities," *Sensors*, vol. 21, no. 21, p. 7099, Oct. 2021. [Online]. Available: https://www.mdpi.com/1424-8220/21/21/7099

[37] Semtech. (2023). *Coexistence of LoRaWAN and UHF RFID*. Accessed: Dec. 20, 2023. [Online]. Available: https://Lora-developers.semtech.com/documentation

[38] A. A. Doroshkin, A. M. Zadorozhny, O. N. Kus, V. Y. Prokopyev, and Y. M. Prokopyev, "Experimental study of LoRa modulation immunity to Doppler effect in CubeSat radio communications," *IEEE Access*, vol. 7, pp. 75721–75731, 2019.

[39] A. M. Zadorozhny, A. A. Doroshkin, V. N. Gorev, A. V. Melkov, A. A. Mitrokhin, V. Y. Prokopyev, and Y. M. Prokopyev, "First flight-testing of LoRa modulation in satellite radio communications in low-Earth orbit," *IEEE Access*, vol. 10, pp. 100006–100023, 2022.

[40] *SALSA Algorithm*. Accessed: Jul. 26, 2023. [Online]. Available: https://github.com/list-luxembourg/salsa

[41] *Python Geocoding Toolbox*. Accessed: Jul. 26, 2023. [Online]. Available: https://pypi.org/project/geopy/

[42] *Elegant Astronomy for Python*. Accessed: Jul. 26, 2023. [Online]. Available: https://pypi.org/project/skyfield/

[43] *CelesTrack Database*. Accessed: Jul. 26, 2023. [Online]. Available: https://celestrak.org/

FELIPE AUGUSTO TONDO received the B.Sc. degree in electrical engineering from the University of Caxias do Sul (UCS), Brazil, in 2014, and the M.Sc. degree in electrical engineering from the Federal University of Rio Grande do Sul, Brazil, in 2017. He is currently pursuing the Ph.D. degree with the Graduate Program of Electrical Engineering, Federal University of Santa Catarina (UFSC), Brazil. Since this year, has held a position as a Professor with the Department of Electrical, Electronic, and Control and Automation Engineering, UCS. His research interest includes wireless communications, specifically with ground-to-satellite networks. He has worked in the efficient resource allocation for IoT networks via low orbit satellites (LEOs). In 2022, he collaborated with Programa Institucional de Fomento a la Investigación, Desarrollo e Innovación, Universidad Tecnológica Metropolitana (UTEM), Santiago, Chile. In 2023, his research project was accepted by the Brazilian National Program for Scientific and Technological Development, leading to an exchange opportunity with the Centre for Wireless Communications (CWC), Oulu, Finland.

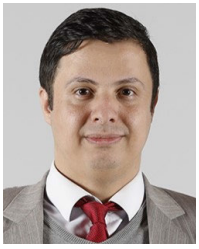

MOHAMMAD AFHAMISIS (Member, IEEE) received the bachelor's degree in telecommunication engineering from Semnan University, Iran, and the Master of Science degree in satellite technology engineering from Iran University of Science and Technology (IUST). He is currently pursuing the Ph.D. degree with Luxembourg Institute of Science and Technology (LIST), ERIN Department, working on optimizing LoRaWAN protocol for integration with satellite for smart agriculture applications. His thesis was on optimizing the control of GEO satellites with large antennas and deployable solar cells. Also, he has six years of experience in working as a Senior Radio Communications Specialist in the Iranian railways headquarter office and managed different radio communications and IoT monitoring projects.

SAMUEL MONTEJO-SÁNCHEZ (Senior Member, IEEE) received the B.Sc., M.Sc., and D.Sc. degrees in telecommunications from the Central University of Las Villas (UCLV), Santa Clara, Cuba, in 2003, 2007, and 2013, respectively. From 2003 to 2017, he was an Associate Professor with UCLV. Now, he is a Full Professor at the Instituto Universitario de Investigación y Desarrollo Tecnológico, Universidad Tecnológica Metropolitana, Santiago, Chile. He led the FONDECYT Postdoctoral No. 3170021 (Transmission Resources Equitable Allocation in Energy-Efficient Wireless Communications) and the FONDECYT Iniciación No. 11200659 (Toward High-Performance Wireless Connectivity for IoT and Beyond-5G Networks) Projects. Furthermore, he participated as a Co-Investigator in the FONDECYT Regular No. 1201893 (IoT goes to Space: Wireless Networking Protocols and Architectures for IoT Networks served by LEO Satellite Constellations). He currently leads the ANID FONDECYT Regular No. 1241977 (In Touch: Intelligent Networks Towards Opportunity, Understanding, Coverage, and Hope). His research interests include wireless communications, signal processing, sustainable IoT, and wireless RF energy transfer. He was a co-recipient of the 2016 Research Award from the Cuban Academy of Sciences and he was a co-supervisor of the awarded Ph.D. Thesis with the 2022 Abertis Award for Research in Road Safety (Ex—Aequo) at the national and international level.

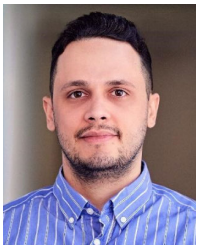

ONEL LUIS ALCARAZ LÓPEZ (Member, IEEE) received a B.Sc. degree (Hons.) from the Central University of Las Villas, Cuba, in 2013, a M.Sc. degree from the Federal University of Paraná, Brazil, in 2017, and a D.Sc. degree (Hons.) in electrical engineering from the University of Oulu, Finland, in 2020. From 2013 to 2015, he was a Specialist in telematics with the Cuban Telecommunications Company (ETECSA). He is currently an Assistant Professorship (tenure track) in sustainable wireless communications engineering with the Centre for Wireless Communications (CWC), Oulu, Finland. He has authored the books titled *Wireless RF Energy Transfer in the Massive IoT Era: Towards Sustainable Zero-Energy Networks* (Wiley, December 2021) and *URLLC: Foundations, Enablers, System Design, and Evolution Towards 6G* (Now Publishers, 2023). His research interests include wireless connectivity, the sustainable and dependable IoT, energy harvesting, wireless RF energy transfer, machine-type communications, and cellular-enabled positioning systems. He is a Collaborator to the 2016 Research Award given by the Cuban Academy of Sciences, a co-recipient of the 2019 and 2023 IEEE European Conference on Networks and Communications (EuCNC) Best Student Paper Award, a recipient of the 2020 Best Doctoral Thesis Award granted by Academic Engineers and Architects in Finland TEK and Tekniska Föreningen i Finland TFiF, in 2021, and a recipient of the 2022 Young Researcher Award in the field of technology in Finland.

MARIA RITA PALATTELLA (Member, IEEE) received the Ph.D. degree. She is currently a Senior Researcher and Technology (R&T) Associate with the Environmental Research and Innovation (ERIN) Department, Luxembourg Institute of Science and Technology (LIST). She is leading the work on the design of innovative communication systems and network architectures for the different Internet of Things (IoT) applications, including environmental monitoring and precision agriculture. She served as a PI and a Project Manager for several national and international projects (FNR LORSAT, SMC Lux5GCloud, IoT4WEED, and H2020 HEMS) investigating the use of the IoT for smart agriculture applications (e.g., crop supervision and weed control). She is the Coordinator of the EU Horizon Europe COMMECT Project, aiming at connecting the unconnected, by designing energy-efficient and cost-effective connectivity solutions for rural and remote areas. In the context of the emerging 6G systems, she has investigated means of efficiently intertwining IoT and satellites, with focus on LoRa/LoRaWAN in the FNR LORSAT Project, and focus on NB-IoT in the SatNEX V ONION Project. Last, but not least, she is the Coordinator of the SatNEX V INVENTIVE Project, investigating IoT Connectivity via multi-layer NTN Encompassing UAVs and LEO Systems. She sits on the Editorial Board of the *Transactions on Emerging Telecommunications Technologies* (ETT), and the *EAI Transactions on IoT*. She was the Secretary of the IEEE 5G Mobile Wireless Internet Technical Subcommittee. She has served as a TPC member for several IoT-related conferences, recently the Tutorial Co-Chair for ICC2024. She is a reviewer for international conferences and journals. She has (co)authored several papers published in well known, high-impact journals and international conferences, and two patents.

RICHARD DEMO SOUZA (Senior Member, IEEE) received the D.Sc. degree in electrical engineering from the Federal University of Santa Catarina (UFSC), Brazil, in 2003. From 2004 to 2016, he was with the Federal University of Technology Paraná (UTFPR), Brazil. Since 2017 he has been with UFSC, where he is currently a Professor with the Department of Electrical and Electronics Engineering. His research interests include the areas of wireless communications and signal processing. He has served as an Editor or an Associate Editor for the *SBrT Journal of Communications and Information Systems*, IEEE COMMUNICATIONS LETTERS, IEEE TRANSACTIONS ON VEHICULAR TECHNOLOGY, IEEE TRANSACTIONS ON COMMUNICATIONS, and IEEE INTERNET OF THINGS JOURNAL. He is a Supervisor of the awarded Best Ph.D. Thesis in Electrical Engineering in Brazil, in 2014. He is a co-recipient of the 2016 Research Award from the Cuban Academy of Sciences.